AMERICAN SOCIETY FOR MICROBIOLOGY | Molecular and Cellular Biology®

RESEARCH ARTICLE

Vitamin K-Dependent γ-Glutamyl Carboxylase in Sertoli Cells Is Essential for Male Fertility in Mice

Sachiko Shiba,[a] Kazuhiro Ikeda,[a] Kuniko Horie-Inoue,[a] Kotaro Azuma,[b] Tomoka Hasegawa,[c] Norio Amizuka,[c] Tomoaki Tanaka,[d] Toshihiko Takeiwa,[a] Yasuaki Shibata,[e] Takehiko Koji,[e] Satoshi Inoue[a,b]

[a]Division of Gene Regulation and Signal Transduction, Research Center for Genomic Medicine, Saitama Medical University, Saitama, Japan
[b]Department of Systems Aging Science and Medicine, Tokyo Metropolitan Institute of Gerontology, Tokyo, Japan
[c]Department of Developmental Hard Tissue, Graduate School of Dental Medicine, Hokkaido University, Sapporo, Hokkaido, Japan
[d]Department of Clinical Cell Biology and Medicine, Graduate School of Medicine, Chiba University, Chiba, Japan
[e]Department of Histology and Cell Biology, Nagasaki University Graduate School of Biomedical Sciences, Nagasaki, Japan

ABSTRACT γ-Glutamyl carboxylase (GGCX) is a vitamin K (VK)-dependent enzyme that catalyzes the γ-carboxylation of glutamic acid residues in VK-dependent proteins. The anticoagulant warfarin is known to reduce GGCX activity by inhibiting the VK cycle and was recently shown to disrupt spermatogenesis. To explore GGCX function in the testis, here, we generated Sertoli cell-specific *Ggcx* conditional knockout (*Ggcx* scKO) mice and investigated their testicular phenotype. *Ggcx* scKO mice exhibited late-onset male infertility. They possessed morphologically abnormal seminiferous tubules containing multinucleated and apoptotic germ cells, and their sperm concentration and motility were substantially reduced. The localization of connexin 43 (Cx43), a gap junction protein abundantly expressed in Sertoli cells and required for spermatogenesis, was distorted in *Ggcx* scKO testes, and Cx43 overexpression in Sertoli cells rescued the infertility of *Ggcx* scKO mice. These results highlight GGCX activity within Sertoli cells, which promotes spermatogenesis by regulating the intercellular connection between Sertoli cells and germ cells.

KEYWORDS γ-glutamyl carboxylase, Sertoli cell, infertility, testis, knockout

Vitamin K (VK) is an essential nutrient that plays roles in blood coagulation and bone homeostasis. Natural VK forms are VK1 and VK2 (1), with the former being converted into the latter *in vivo* (2, 3). As one of the major functions of VK, it behaves as a cofactor for γ-glutamyl carboxylase (GGCX), which catalyzes a posttranslational modification of a glutamic acid (Glu) residue into a γ-carboxyglutamic acid (Gla) residue (4). This γ-carboxylation is a critical protein modification for VK-dependent proteins involved in physiological processes, including blood coagulation, fibrinolysis, and bone homeostasis (3, 5, 6).

In humans and mice, the GGCX protein is localized in the endoplasmic reticulum, with 3 potential Gla modification sites in its amino acid residues (5). Clinically, loss-of-function *GGCX* mutations exhibit the deficient activity of VK-dependent coagulation factors, leading to bleeding disorders (7, 8). In contrast, a gain-of-function *GGCX* polymorphism is associated with high bone mineral density in elderly women (9). Regarding the loss of function of GGCX in mice, conventional *Ggcx* knockout (KO) mice exhibited peripartum lethality (10). To dissect the tissue-specific activity of GGCX, we previously generated conditional *Ggcx* KO (cKO) mice by crossing mice harboring a conditional *Ggcx* allele by flanking exon 6 of the *Ggcx* gene with loxP sites (*Ggcx* floxed) with tissue-specific Cre recombinase-expressing mice (4). Liver-specific *Ggcx*-deficient mice exhibited a shorter life span due to bleeding diathesis, showing that GGCX is required for the activities of coagulation factors II and IX (4). In addition,

Citation Shiba S, Ikeda K, Horie-Inoue K, Azuma K, Hasegawa T, Amizuka N, Tanaka T, Takeiwa T, Shibata Y, Koji T, Inoue S. 2021. Vitamin K-dependent γ-glutamyl carboxylase in Sertoli cells is essential for male fertility in mice. Mol Cell Biol 41:e00404-20. https://doi.org/10.1128/MCB.00404-20.

Address correspondence to Satoshi Inoue, sinoue@tmig.or.jp.

Received 7 August 2020
Returned for modification 8 September 2020
Accepted 24 January 2021
Accepted manuscript posted online 1 February 2021
Published 24 March 2021

osteoblast-specific *Ggcx*-deficient mice revealed that GGCX regulates bone mineralization and glucose metabolism (11–15).

As GGCX activity is dependent on VK levels, the anticoagulant warfarin reduces GGCX activity by blocking VK epoxide reductase (VKOR) complex subunit 1 (VKORC1) and inhibiting the VK cycle (16). In a study using rats with daily intake of a low dose of warfarin, endogenous substrates for GGCX accumulated in various tissues, including the testes, lungs, spleen, and liver (17). Warfarin also suppresses dithiothreitol-dependent VKOR activity in the testes, liver, and kidney (18). Recent studies have revealed that warfarin also exerts negative effects on spermatogenesis (19, 20). Based on these findings, we questioned whether testis-specific loss of function of GGCX directly causes disorders of spermatogenesis.

In the present study, we generated Sertoli cell-specific *Ggcx* cKO (scKO) mice by crossing transgenic mice expressing anti-Müllerian hormone (*AMH*) gene promoter-driven Cre recombinase (*AMH-Cre*) (21, 22) with *Ggcx*-floxed mice (4, 14, 15). Our study aimed to examine the physiological role of VK-dependent GGCX in Sertoli cells, which are essential for testis formation and spermatogenesis (23). *Ggcx* scKO male mice exhibited infertility with atrophy of seminiferous tubules and sperm cells. Notably, the expression of the gap junction protein connexin 43 (Cx43) was distorted in Sertoli cells of *Ggcx* scKO mice. Our results indicate that VK-dependent GGCX in Sertoli cells is a critical regulator of spermatogenesis.

RESULTS

Generation of Sertoli cell-specific *Ggcx*-deficient mice. To examine the testis-specific activity of GGCX, we generated Sertoli cell-specific *Ggcx* cKO (scKO) mice by crossing *AMH-Cre* transgenic mice with *Ggcx*-floxed mice (4, 14, 15). In *AMH-Cre* mice, Sertoli cell-specific *AMH-Cre* expression was shown by crossing them with *ROSA26-LacZ* reporter mice (Fig. 1A). Male *Ggcx* scKO (*AMH-Cre*; $Ggcx^{flox/flox}$) mice were generated by mating male and female *AMH-Cre*; $Ggcx^{flox/+}$ mice. For genotyping, the *Cre* recombinase gene (654 bp) was amplified by the primers generated in it by PCR using genomic DNA prepared from the tail (4). The intact (wild-type [WT]) (407-bp) and *loxP*-containing (floxed) (454-bp) exons 5 of the *Ggcx* gene were also amplified for genotyping the *Ggcx* allele (4) (Fig. 1B). *AMH-Cre*; $Ggcx^{+/+}$ (*AMH-Cre*) or $Ggcx^{+/+}$ (WT) mice were used as controls in further experiments.

In the *Ggcx* scKO testes, quantitative reverse transcriptase PCR (qRT-PCR) showed that *Ggcx* mRNA expression was barely detectable at 2 months of age (Fig. 1C). GGCX protein levels were also substantially decreased in the *Ggcx* scKO testes compared to those of controls based on Western blot analysis (Fig. 1D) and immunohistochemical analysis (Fig. 1E).

***Ggcx* scKO mice exhibit late-onset male infertility.** We found that *Ggcx* scKO male mice exhibit infertility during the generation of *Ggcx* scKO mice. To further monitor breeding capacity, *Ggcx* scKO male mice were mated with WT females (Table 1). Although 2-month-old *Ggcx* scKO male mice were fertile to produce pups, 3- and 6-month-old *Ggcx* scKO male mice did not exhibit reproductive abilities, while copulatory plugs were observed in the mated WT females. These results indicate that *Ggcx* depletion in Sertoli cells causes late-onset male infertility. In contrast, male $Ggcx^{flox/flox}$ mice (without *Cre*) and female *Ggcx* scKO mice had normal reproductive abilities. Notably, the *Ggcx* scKO male mice had apparently smaller testes than control mice at 2, 4, and 8 months of age (Fig. 2A to C). The difference in the testis weights was statistically significant between *Ggcx* scKO and control mice at the examined age (Fig. 2D to F). Serum testosterone levels, however, did not exhibit significant differences between *Ggcx* scKO male and *AMH-Cre* mice (Table 2).

Histological abnormality in *Ggcx* scKO testes. We next examined testicular histology by hematoxylin and eosin (HE) staining (Fig. 3A). Although the 2-month-old *Ggcx* scKO mice exhibited nearly normal testicular histology, their testis size was smaller than that of *AMH-Cre* mice. In contrast, drastic histological abnormality was detected in *Ggcx* scKO testes at both 4 and 8 months of age. The 4-month-old *Ggcx* scKO testes

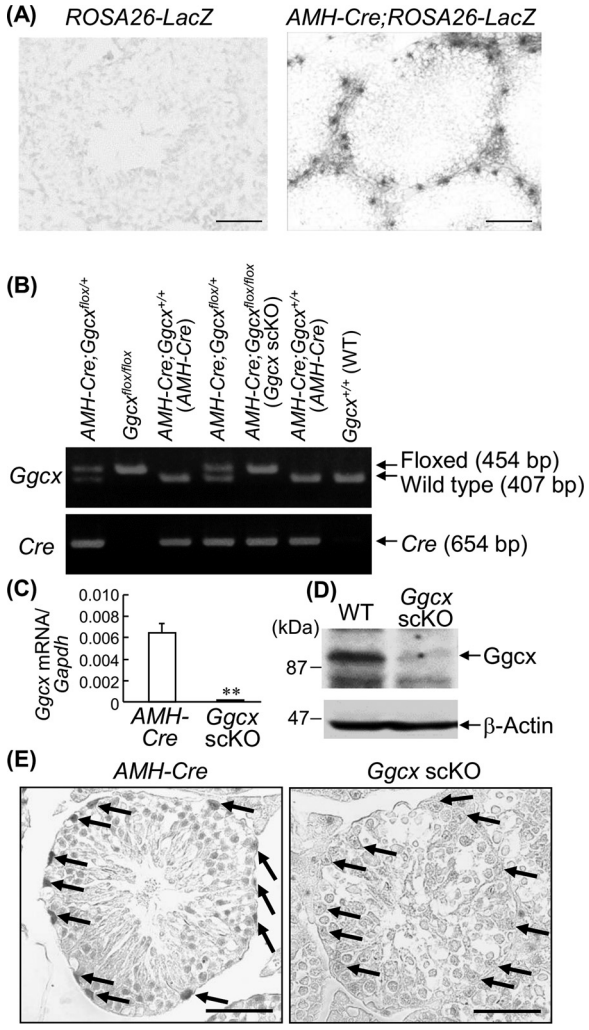

FIG 1 Generation of Sertoli cell-specific *Ggcx*-deleted mice. (A) *AMH* gene expression in the Sertoli cells of male *AMH-Cre*; *ROSA26-LacZ* mice was visualized by β-galactosidase staining. *In vivo* recombination of the *Rosa26-LacZ* locus is mediated by the Cre transgene product. Bars, 20 μm. (B) Generation of *AMH-Cre*; $Ggcx^{flox/flox}$ (*Ggcx* scKO) mice. *Ggcx*-floxed and *AMH-Cre* mice were crossed to generate *AMH-Cre*; $Ggcx^{flox/flox}$ (*Ggcx* scKO) mice. Genotyping was performed using genomic DNA extracted from tails using primer pairs that were derived from the 5′- and 3′-flanking sequences of the loxP sequence (top) and *Cre* recombinase (bottom). *AMH-Cre*; $Ggcx^{+/+}$ mice were used as control animals in the experiments. (C) Ablation of *Ggcx* mRNA expression in *Ggcx* scKO testes. Expression levels of *Ggcx* mRNA were quantified by qRT-PCR in testes from 2-month-old *Ggcx* scKO and *AMH-Cre* mice. Data are presented as means $\pm$ standard errors of the means (SEM) ($n = 3$). **, $P < 0.01$ (using Student's *t* test). (D) Deletion of GGCX protein expression in *Ggcx* scKO testes. Western blot analysis of GGCX was performed in testes from 2-month-old *Ggcx* scKO and WT mice. β-Actin antibody was used as a loading control. (E) Sertoli cell-specific deletion of GGCX expression in *Ggcx* scKO mice. Immunohistochemical analyses of GGCX in testes were performed in 4-month-old *Ggcx* scKO and *AMH-Cre* mice. The arrows indicate Sertoli cells. Bars, 20 μm.

exhibited large multinuclear spermatids and intercellular space. The 8-month-old *Ggcx* scKO testes exhibited large clear lumen regions of the seminiferous tubules with severely decreased spermatids. Further analysis by transmission electron microscopy (TEM) revealed that the multinuclear spermatids possess chromatin aggregation, nuclear fragmentation, vacuoles, and destroyed organelles, implicating apoptotic features (Fig. 3B) (24, 25).

Increased apoptosis in *Ggcx* scKO testes. To assess whether apoptosis predominantly occurred in *Ggcx* scKO testes, a terminal deoxynucleotidyltransferase (TdT)-mediated dUTP-biotin nick end labeling (TUNEL) assay was performed on testis

TABLE 1 Fertility evaluation of male *Ggcx* scKO mice[a]

Age of males (mo)	No. of mated pairs	No. of pregnancies	No. of litters	Avg litter size
2	2	1	5	5
3	6	0	0	NA
6	6	0	0	NA

[a]Individual male *Ggcx* scKO mice ($n = 2$ at 2 months of age, and $n = 3$ at 3 and 6 months of age) were mated with one or two WT (C57BL/6) females for 3 months. NA, not applicable.

sections of 2-, 4-, and 8-month-old mice (Fig. 4A). While TUNEL-labeled spermatogenic cells were observed in *AMH-Cre* mouse testes throughout the examined period, the counts of labeled cells were significantly increased in age-matched *Ggcx* scKO mouse testes (Fig. 4B). Large TUNEL-positive spermatocytes were especially observed in *Ggcx* scKO mouse testes (Fig. 4A). In addition, we examined the expression levels of proapoptotic *Bax* and antiapoptotic *Bcl2* in 8-month-old *AMH-Cre* and *Ggcx* scKO testes (Fig. 4C). *Bax* expression and *Bax*/*Bcl2* ratios were significantly elevated in *Ggcx* scKO compared with *AMH-Cre* mice.

Abnormal spermatozoa in *Ggcx* scKO mouse testes. We then analyzed the phenotype of spermatozoa prepared from the epididymis. The sperm concentration was significantly decreased in the *Ggcx* scKO mice compared to *AMH-Cre* mice (Fig. 5A). In addition, the populations of morphologically abnormal spermatozoa were significantly increased in *Ggcx* scKO mice compared with control mice, exhibiting phenotypes with a disordered flagellum and sperm head, as exemplified by a coiled tail, bent neck, and abnormal head (Fig. 5B). In the sperm motility analysis, the percentage of normal hyperactive sperm cells of *Ggcx* scKO mouse testes was decreased to half of that of *AMH-Cre* mouse testes (Fig. 5C). In contrast, irregularly moving sperm cells were drastically increased in *Ggcx* scKO mouse testes compared to *AMH-Cre* mouse testes. However, a spontaneous acrosome reaction of spermatozoa was similarly found in *AMH-Cre* (2.38- $\pm$ 1.84-fold) and *Ggcx* scKO (2.42- $\pm$ 0.92-fold) mice during capacitation incubation, suggesting no apparent defect in sperm capacitation.

Abnormal expression and localization of connexin 43 in *Ggcx* scKO Sertoli cells. To further define the physiological characteristic of Sertoli cells in *Ggcx* scKO mouse testes, we performed immunohistochemical analysis for the transcriptional factor GATA1 and the gap junction protein connexin 43 (Cx43). GATA1 is known as a Sertoli cell-specific marker that functions as a developmental stage- and spermatogenic cycle-specific regulator of gene expression (26, 27). Cx43 is a predominant testicular gap

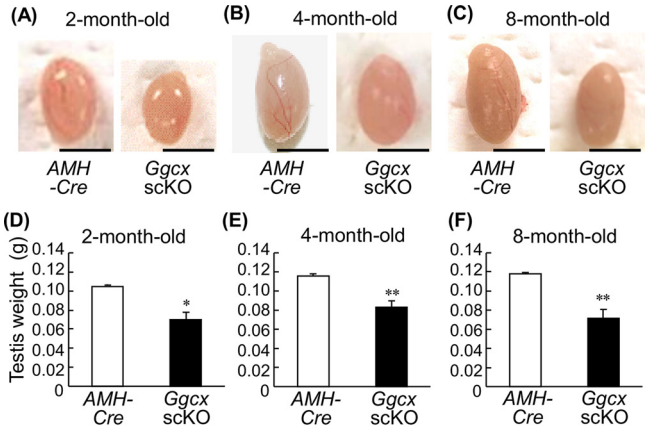

FIG 2 Decreased testis size in *Ggcx* scKO mice. The appearance (A to C) and weight (D to F) of testes were examined in *Ggcx* scKO and *AMH-Cre* mice at 2 months (A and D), 4 months (B and E), and 8 months (C and F) of age. Data are presented as means $\pm$ SEM ($n = 3$). *, $P < 0.05$; **, $P < 0.01$ (using Student's *t* test). Bars, 5 mm.

TABLE 2 Serum testosterone levels in male *Ggcx* scKO and control mice[a]

	Mean serum testosterone level (ng/ml) ± SEM	
Age (mo)	Control	*Ggcx* scKO
2	20.29 ± 8.46	9.75 ± 7.15
4	12.46 ± 6.70	18.88 ± 7.57
8	24.29 ± 2.43	22.00 ± 6.32

[a]*n* = 3 mice/group. The *P* values were not significant.

junction protein and plays an essential role in spermatogenesis but not spermatogonial maintenance/proliferation in Sertoli cells (28). GATA1-positive signals in *Ggcx* scKO testes were basically equal to those in *AMH-Cre* testes (Fig. 6A). While Cx43-positive signals were substantially observed at the basal side of Sertoli cells in *AMH-Cre* testes, those in *Ggcx* scKO mice were distorted, particularly at 4 and 8 months of age (Fig. 6B). The signals were slightly moved to the inner side of the seminiferous tubules in 4-month-old *Ggcx* scKO mouse testes, and their intensity was substantially reduced in 8-month-old *Ggcx* scKO mouse testes. Taken together, the expression and localization of Cx43 were disordered in Sertoli cells of *Ggcx* scKO mouse testes. However, the mRNA levels of *Gata1* and *Cx43*, in addition to *Gata4*, were not substantially different between *AMH-Cre* and *Ggcx* scKO mice (Fig. 6C), implying that the transcription of these genes is not primarily regulated by *Ggcx*-mediated signaling pathways.

Cx43 overexpression rescues the pathological testicular phenotype of *Ggcx* scKO mice. Because Cx43 plays a role in testicular germ cell development and differentiation (29), we further investigated whether Cx43 overexpression in Sertoli cells of *Ggcx* scKO mice rescues their infertility. We generated transgenic mice expressing C-terminally Flag-tagged Cx43 under the control of the *AMH* promoter (*AMH-Cx43-Flag*) (Fig. 7A and B). The *AHM-Cx43-Flag* mice expressed the *Cx43-Flag* transgene in the testes (Fig. 7C). *AMH-Cx43-Flag* mice were then crossed with *Ggcx* scKO mice to generate *AMH-Cx43-Flag*; *Ggcx* scKO mice. In *AMH-Cx43-Flag*; *Ggcx* scKO testis, the *Ggcx* level

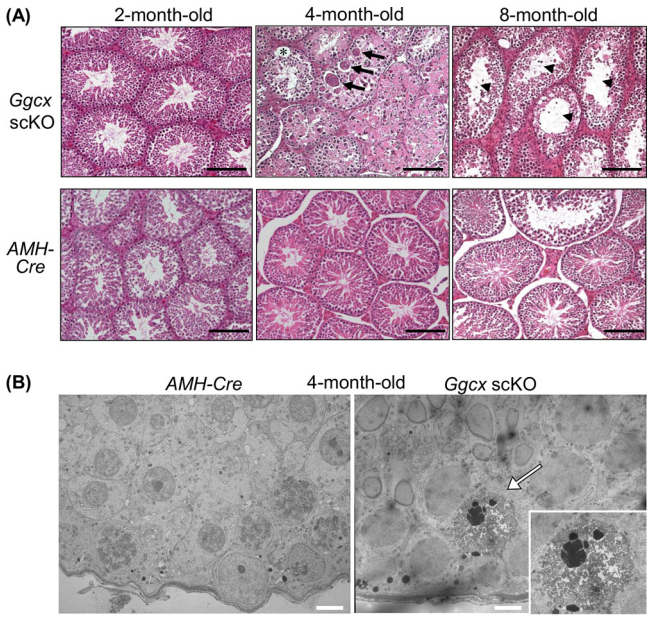

FIG 3 Histological anomaly in *Ggcx* scKO testis. Hematoxylin and eosin (HE) staining (A) and transmission electron microscopic analysis (B) of testes were performed in *Ggcx* scKO and *AMH-Cre* mice. In panel A, arrows and arrowheads indicate large multinuclear spermatids and intercellular space in seminiferous tubules, respectively. Bars, 50 μm. In panel B, the arrow indicates apoptotic alteration of multinuclear spermatids. The inset shows a higher-magnification image. Bars, 5 μm.

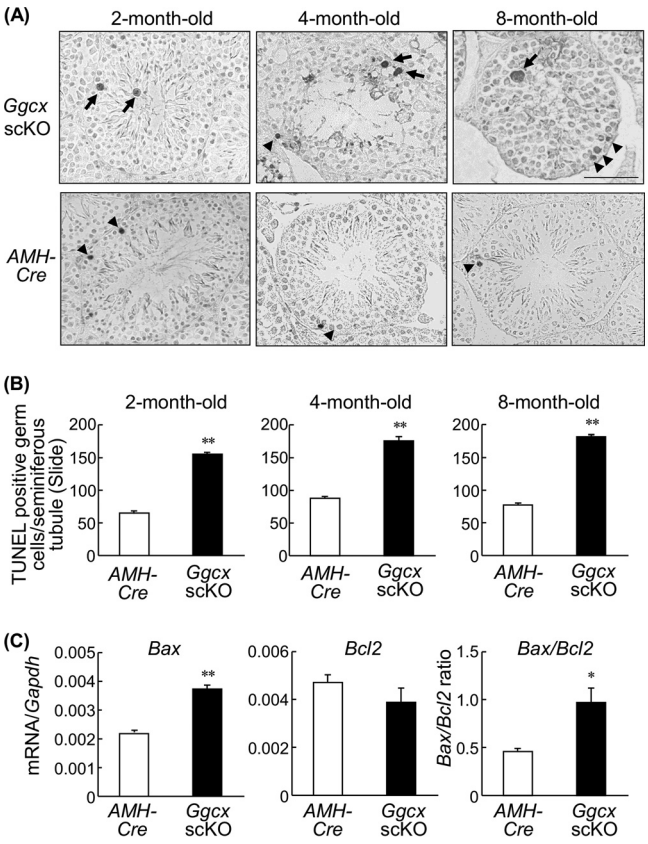

FIG 4 Increase of TUNEL-positive cells in *Ggcx* scKO testes. (A) TUNEL staining of the testis paraffin sections from 2-, 4-, and 8-month-old *Ggcx* cKO and *AMH-Cre* mice. Arrowheads indicate TUNEL-labeled spermatogenic cells observed in both *AMH-Cre* and *Ggcx* scKO mice. Arrows indicate large TUNEL-positive spermatocytes that are observed predominantly in *Ggcx* scKO testes. (B) Number of TUNEL-positive cells. (C) Expression levels of *Bax* and *Bcl2* mRNAs were quantified by qRT-PCR in 8-month-old *Ggcx* cKO and *AMH-Cre* mouse testes. Data are presented as means ± SEM ($n = 3$). *, $P < 0.05$; **, $P < 0.01$ (using Student's *t* test).

was similar to that in *Ggcx* scKO mice and significantly lower than those in WT and *AMH-Cx43-Flag* mice, indicating adequate testicular *Ggcx* ablation in crossing *Ggcx* scKO mice with *AMH-Cx43-Flag* mice (Fig. 7D). Fertility analysis revealed that male *AMH-Cx43-Flag*; *Ggcx* scKO mice have reproductive abilities, indicating that Cx43 overexpression in Sertoli cells recovers the sterility of *Ggcx* scKO mice (Table 3). The testis size and weight of *AMH-Cx43-Flag*; *Ggcx* scKO mice at 8 months of age were not significantly different from those of WT and *AMH-Cx43-Flag* mice (Fig. 7E and F). Moreover, no apparent abnormality was observed in the testicular histology of *AMH-Cx43-Flag*; *Ggcx* scKO mice at 8 months of age compared with the testicular histology of *Ggcx* scKO mice with multinuclear spermatids and large clear lumen regions (Fig. 7G). Moreover, immunohistochemical analysis demonstrated that the Cx43 protein distribution in *Ggcx* scKO testis rescued by Cx43 was recovered to a level similar to that in WT or *AMH-Cx43-Flag* mice (Fig. 7H).

DISCUSSION

In the present study, we generated Sertoli cell-specific *Ggcx* knockout (*Ggcx* scKO) mice and analyzed the role of GGCX in spermatogenesis. The *Ggcx* scKO mice exhibited late-onset male infertility. Histologically, their testes showed substantial atrophy in seminiferous tubules and increased apoptotic degeneration of spermatids and spermatocytes. Decreased concentration and motility were observed in sperm cells prepared

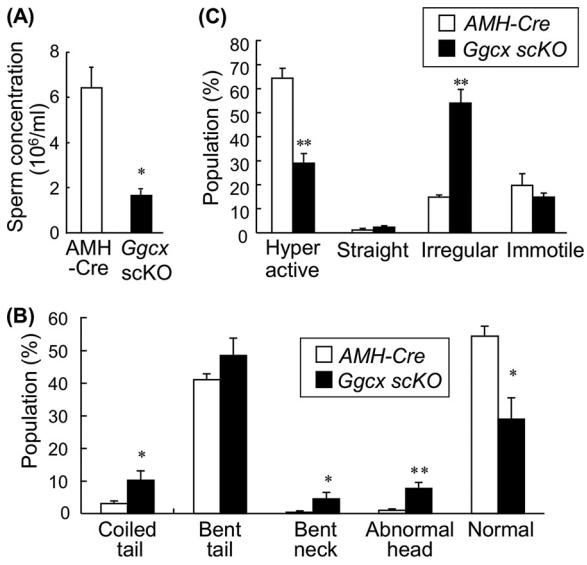

FIG 5 Abnormal phenotype of spermatozoa in *Ggcx* scKO mice. (A) Sperm concentration from cauda epididymides in *Ggcx* scKO and control mice. Sperm cells were recovered from the cauda epididymides of 4-month-old *Ggcx* scKO ($n = 3$) and *AMH-Cre* ($n = 3$) mice. (B) Morphological analysis of sperm cells. Morphological abnormalities of sperm cells were classified into 4 categories: round tail, bent midpiece, bent head, and unclear head. At least 100 sperm cells per mouse were examined. (C) Sperm motility analysis. Sperm motility was categorized by either hyperactive, straight, irregular, or immotile sperm. At least 100 sperm cells per mouse were counted. Data are presented as means ± SEM ($n = 3$). *, $P < 0.05$, **, $P < 0.01$ (using Student's *t* test).

from the epididymis of *Ggcx* scKO mice. Our results reveal that GGCX in Sertoli cells plays a crucial role in spermatogenesis.

In seminiferous tubules, the interface between adjacent Sertoli cells near the basement membrane consists of the immunological barrier system called the blood-testis barrier (BTB) by specialized junctions, including desmosomes, gap junctions, and tight junctions (30). Sertoli cells exert essential functions in testicular differentiation and development in embryos by producing AMH, which causes developmental regression of Müllerian ducts (31). In adults, Sertoli cells function as supporting or nursing cells for testicular germ cells in spermatogenesis (32, 33). The actin-based anchoring cell-cell junction between Sertoli cells and germ cells at the stage of the seminiferous epithelium cycle is especially known as apical ectoplasmic specialization (ES) (30), which structurally provides a spermatogenic niche that regulates the migration and release of germ cells (33–35). The junctions between adjacent Sertoli cells also comprise the basal ES at the BTB, along with desmosomes, gap junctions, and tight junctions (30). Spermatocytes translocate to the adluminal compartment via the BTB at specific seminiferous epithelial cycle stages (36). Considering that Sertoli cells are the main component in the BTB and ES, we assume that GGCX and its substrates in Sertoli cells exert particular functions in spermatogenesis.

Cx43 is a major type of connexin in the testes and predominantly expressed in Sertoli cells (37). Cx43 comprises gap junctions that are located in the apical ES between Sertoli cells and germ cells, including spermatogonia and primary spermatocytes (38, 39). The loss of Sertoli cell-specific Cx43 in mice clarified that Cx43 is necessary for normal testicular development and spermatogenesis (28, 29, 40, 41). Sertoli cell-specific *Cx43* KO mice exhibited smaller testicular sizes and weights, reductions of spermatogonia, and increases in apoptotic germ cells, leading to spermatogenic arrest. Because the testicular phenotype of Sertoli cell-specific *Cx43* KO mice exhibits similarity compared with that of *Ggcx* scKO mice in our study, we assume that a loss of function of GGCX may impair the function of Cx43 in the gap junctions of Sertoli cells and germ cells or the BTB system.

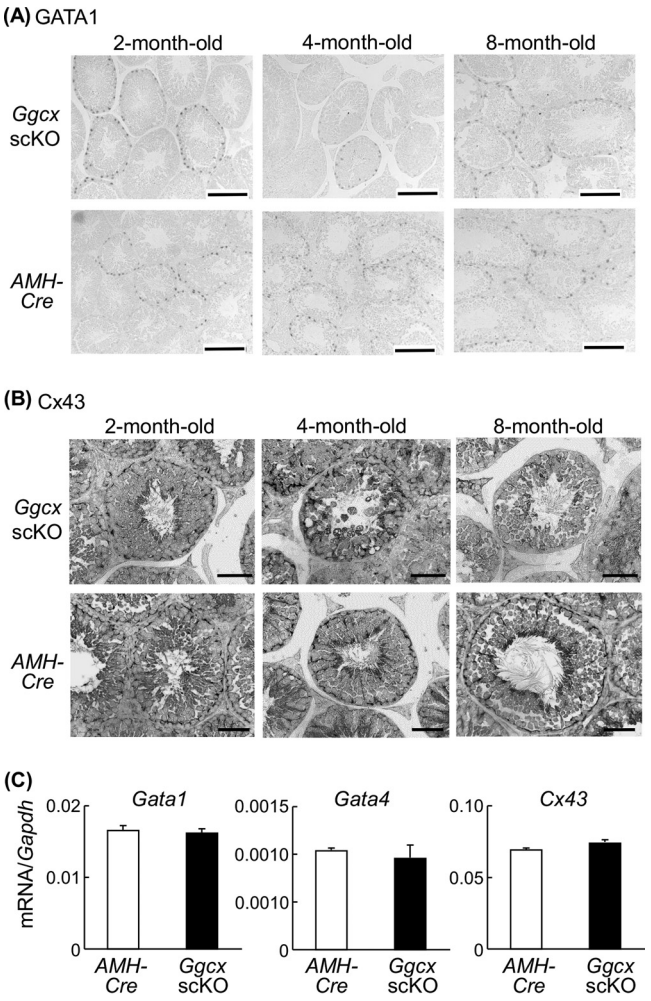

FIG 6 Expression of Sertoli cell-specific markers GATA1, GATA4, and connexin 43 (Cx43) in *Ggcx* scKO testes. (A and B) Immunohistochemistry of GATA1 (A) and Cx43 (B) was performed on testicular sections of *Ggcx* scKO and *AMH-Cre* mice. Bars, 100 μm for Gata1 and 50 μm for Cx43. (C) Expression levels of *Gata1*, *Gata4*, and *Cx43* mRNAs were quantified by qRT-PCR in 8-month-old *Ggcx* cKO and *AMH-Cre* mouse testes. Data are presented as means ± SEM ($n = 3$).

Intriguingly, *AMH-Cx43-Flag*; *Ggcs* scKO mice in the present study exhibited a phenotype with normal histology of seminiferous tubules and male fertility, indicating that Cx43 overexpression in Sertoli cells can rescue the loss of function of GGCX in *Ggcx* KO mice. Our results indicated that the expression levels of *Cx43* mRNA are not significantly changed between the testes of 8-month-old WT and *Ggcx* scKO mice. In addition, *Ggcx* scKO testes with Cx43 overexpression (*AMH-Cx43-Flag*; *Ggcx* scKO) exhibited normal testis morphology and Cx43 tissue distribution, suggesting that Cx43 overexpression would recover the physiological functions of Sertoli cells. Based on these results, we speculate that the aberrant distribution of Cx43 protein in *Ggcx* scKO testes originates from the abnormality of Sertoli cell morphology and functions due to the *Ggcx* ablation rather than from the undercarboxylation of Gla residues in the Cx43 protein.

On the other hand, elevated *Bax* expression levels and *Bax*/*Bcl2* ratios were found in *Ggcx* scKO mouse testes compared with those in WT mice. It has been reported that the imbalance of the *Bax*/*Bcl2* ratio due to the upregulation of *Bax* and the downregulation of *Bcl2* was substantially associated with germ cell apoptosis mediated by oxidative stress in a study of male mice orally administered T-2 toxin (42). We speculate that

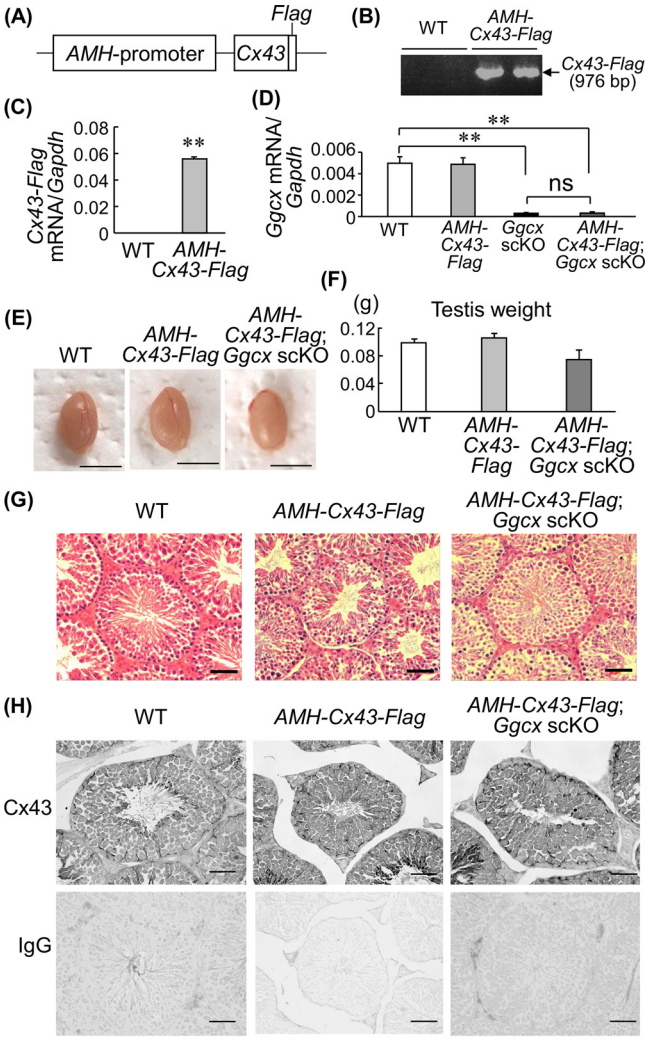

FIG 7 Cx43 rescues the *Ggcx* scKO phenotype. (A) Schematic of the AMH promoter-driven C-terminally Flag-tagged *Ggcx* (*AMH-Cx43-Flag*) transgene. (B) Generation of *AMH-Cx43-Flag* mice. Genotyping was performed using genomic DNA extracted from tails, using primer pairs that were derived from the *AMH* promoter and *Cx43* and *Flag* sequences. (C) Expression levels of the *Cx43-Flag* transgene were quantified by qRT-PCR in testes from 2-month-old *AMH-Cx43-Flag* and WT mice. (D) *Ggcx* levels in WT, *AMH-Cx43-Flag*, *Ggcx* scKO, and *AMH-Cx43-Flag*; *Ggcx* scKO mouse testes. *Ggcx* expression levels were quantified by qRT-PCR in the testes from 8-month-old mice. Data are presented as means ± SEM ($n = 3$). **, $P < 0.01$ (using Student's *t* test). ns, not significant. (E) Representative testes of WT, *AMH-Cx43-Flag*, and *AMH-Cx43-Flag*; *Ggcx* scKO mice at 8 months of age. Bars, 5 mm. (F) Testis weights of WT, *AMH-Cx43-Flag*, and *AMH-Cx43-Flag*; *Ggcx* scKO mice at 8 months of age. Data are presented as means ± SEM ($n = 3$). (G and H) HE staining (G) and immunohistochemistry of Cx43 (H) of testes from 8-month-old WT, *AMH-Cx43-Flag*, and *AMH-Cx43-Flag*; *Ggcx* scKO mice. Immunohistochemistry using normal IgG instead of the antibody is also shown. Bars, 50 μm.

the aberrant activation of the mitochondrial apoptosis pathway may be upregulated in spermatogenesis of *Ggcx* scKO mice.

In *Ggcx* scKO mice, severely impaired seminiferous tubules were observed only after 2 months of age, suggesting that the function of GGCX in Sertoli cells is particularly rel-

TABLE 3 Fertility evaluation of male *AMH-Cx43-Flag*; *Ggcx* scKO mice[a]

Age of males (mo)	No. of mated pairs	No. of pregnancies	No. of litters	Avg litter size
2	2	2	12	6.0
8	2	2	13	6.5

[a]Individual male *AMH-Cx43-Flag*; *Ggcx* scKO mice ($n = 2$ at 2 and 8 months of age) were mated with one WT (C57BL/6) female for 3 months.

evant to sex maturation. During puberty, the major androgen hormone testosterone in testis is produced by Leydig cells. Testosterone is considered to play critical roles in the spermatogenesis process, including in the maintenance of the BTB, Sertoli cell-spermatid adhesion, meiosis, and sperm release (43). Androgen receptor (AR) facilitates BTB remodeling, which is necessary to transmit germ cells from the basal compartment to the adluminal compartment to complete meiosis (44). Because germ cells do not express AR (45–48), it is likely that testosterone acts on AR-expressing cells in seminiferous tubules, such as Sertoli cells, in a paracrine fashion. Notably, Sertoli cell-specific AR knockout male mice exhibited reduced testis weight with no elongated spermatids and germ cell arrest during meiosis (49, 50). In AR hypomorphic mice with decreased AR activity, Sertoli cells could not maintain their adhesive connection to elongated spermatids, thereby inducing premature release and spermatid loss (51). As a recent study revealed that AR is a substrate for γ-carboxylation (52), GGCX may affect puberty by modulating androgen signaling.

As other known GGCX targets, Gas6 and protein S may also be involved in the development of germ cells because these Gla-modified proteins are produced by Leydig cells before sexual maturity and by both Leydig and Sertoli cells thereafter (53). The Tyro3, Axl, and Mer (TAM) receptor tyrosine kinases are receptors for Gas6 and protein S, and triple-knockout mice that lack all three TAM receptors (TAM TKO mice) demonstrate azoospermia and possess abnormal seminiferous tubules that are filled with apoptotic germ cells (53). All three TAM receptors and both of their ligands are expressed in Sertoli cells, and the conjunctive activation of TAM receptors is crucial for the phagocytosis of apoptotic germ cells during spermatogenesis. We assume that a prototypic Gla-containing protein, Gas6, could be a relevant substrate of GGCX in testis, as its function in Sertoli cells has been shown to remove apoptotic cells by binding to the Tyro3 subfamily of the receptor tyrosine kinases Tyro3 and Axl (54). We speculate that the enhancement of apoptosis in *Ggcx* scKO testis could be partly due to the increase in undercarboxylated Gla-modified Gas6, leading to the reduction of the elimination of apoptotic cells by Sertoli cells.

Interestingly, these degenerative phenotypes of TAM TKO mice were found after 5 weeks of age ~1 week after the onset of active sperm production (53). Thus, it is implied that GGCX regulates spermatogenesis cooperatively with androgen signaling. TAM receptor tyrosine kinases also play important roles in the phagocytosis process of apoptotic cells in adult testes (55). Consistent with our findings, the GGCX-Gas6/protein S-TAM axis contributes to phagocytosis in Sertoli cells.

In spermiogenesis, GGCX and its known substrate matrix Gla protein (MGP) colocalized in vesicular structures of the epithelial cell cytoplasm and spermatozoon surface in the epididymal lumen, as analyzed in a warfarin-treated rat study (19). Carboxylated MGP reduces the calcium concentration in epididymal fluid, which is critical for normal spermiogenesis. Thus, the intercellular communication network constructed by vesicle-mediated transport and membrane trafficking may play an important role in spermiogenesis in the epididymis. Although MGP expression is relatively low in the testis, MGP might also play a role in Sertoli cells.

MATERIALS AND METHODS

Generation of *AMH-Cre* and *AMH-Cx43-Flag* mice and genotyping. All animal experiments were approved by the Animal Care and Use Committee of the Saitama Medical University. Mice were maintained in a temperature-controlled room (23°C) with a 12-h-light/dark schedule and fed a standard diet (CE2; Clea Japan, Tokyo, Japan) with free access to water. The $LPANH_3$ plasmid that contains the human *AMH* gene promoter was kindly provided by Jean-Yves Picard (21). The *AMH* promoter region (3.6 kb) was inserted into pxCANCre by exchanging the CAG (cytomegalovirus enhancer, chicken β-actin promoter, and rabbit β-globin splice acceptor site) promoter (56). The resulting *AMH-Cre* plasmid was linearized by restriction enzyme digestion and microinjected into the pronuclei of fertilized eggs from C57BL/6 mice, as previously described (57). *AMH-Cre* transgenic mice were identified by a PCR assay of the genomic DNA using primers for Cre (4). In addition, the same *AMH* promoter region and C-terminally Flag-tagged mouse Cx43 cDNA were inserted into pcDNA3 (Invitrogen, Carlsbad, CA, USA) by exchanging the cytomegalovirus (CMV) promoter. The resulting *AMH-Cx43-Flag* plasmid was used to generate *AMH-Cx43-Flag* transgenic mice. The *AMH-Cx43-Flag* transgenic mice were identified by a PCR assay of

the genomic DNA using primers that are specific to the *AMH* promoter and Cx43 cDNA (5′-AGAGATGGCTGTACCTTGGAGAT-3′ and 5′-CAATCCCATACTTGAACTTCTTGAT-3′, respectively).

Generation of Sertoli cell-specific *Ggcx*-deficient (*AMH-Cre*; *Ggcx*$^{flox/flox}$ scKO) mice and genotyping. *Ggcx*-floxed mice and their genotyping were previously described (4, 14, 15). *AMH-Cre* mice were mated with *Ggcx*$^{flox/flox}$ mice, and their offspring were subsequently intercrossed to generate Sertoli cell-specific *Ggcx*-deficient (*Ggcx*$^{flox/flox}$; *AMH-Cre* scKO) mice.

Fertility assay. Individual male *Ggcx* scKO ($n = 2$ at 2 months of age, and $n = 3$ at 3 and 6 months of age) and *AMH-Cx43*; *Ggcx* scKO ($n = 2$ at 2 and 8 months of age) mice were mated with one or two WT (C57BL/6) females for 3 months. C57BL/6 mice were purchased from Clea Japan.

β-Galactosidase staining. *ROSA26-LacZ* reporter mice were obtained from the Jackson Laboratory (4). Sertoli cell-specific expression of Cre recombinase was confirmed by mating *AMH-Cre* mice with *ROSA26-LacZ* mice. β-Galactosidase staining of the testes was performed, as previously described (22). Briefly, frozen sections of the testes were incubated in phosphate-buffered saline (PBS) containing 2 mM $MgCl_2$, 5 mM $K_3Fe(CN)_6$, 5 mM $K_4Fe(CN)_6$, and 20 mM 5-bromo-4-chloro-3-indolyl-β-D-galactoside (X-gal) at 37°C for 20 h. The sections were counterstained with orange G.

Quantitative reverse transcriptase PCR. Total RNAs were extracted from the testes using Isogen reagent (Nippon Gene, Tokyo, Japan). To investigate the gene expression of *Ggcx*, *Cx43*, *Bax*, and *Bcl2*, quantitative reverse transcriptase PCR (qRT-PCR) was performed as previously described (58). First-strand cDNA generated from the total RNA was subjected to qRT-PCR using the SYBR green PCR master mix (Applied Biosystems, Foster City, CA) and the ABI Prism 7000 system (Applied Biosystems). The sequences of PCR primers are as follows: 5′-TTCATCGCGGGTGTGAAGA-3′ (forward) and 5′-CTCCGACAACACCAGCTTGAA-3′ (reverse) for *Ggcx*, 5′-GAACTCCAGCCCTTAGCTATCGT-3′ (*Cx43* forward) and 5′-TTATTTGTCATCATCATCG TCCTTATAGTC-3′ (*Flag* reverse) for C-terminally Flag-tagged *Cx43*, 5′-CTCACCTATGTCTCCTCCTGGG-3′ (forward) and 5′-GGGAGTTGGAGATGGTGCTTC-3′ (reverse) for *Cx43*, 5′-GCTGCAGACATGCTGTGGATC-3′ (forward) and 5′-TCACAGCCAGGAGAATCGCAC-3′ (reverse) for *Bax*, 5′-ACCGTCGTGACTTCGCAGAG-3′ (forward) and 5′-GGTGTGCAGATGCCGGTTCA-3′ (reverse) for *Bcl2*, 5′-GTCAGAACCGGCCTCTCATC-3′ (forward) and 5′-GGTGCCTGCCCGTTTG-3′ (reverse) for *Gata1*, 5′-CCTGGAAGACACCCCAATCTC-3′ (forward) and 5′-GCCCCACAATTGACACACTCT-3′ (reverse) for *Gata4*, and 5′-GCATGGCCTTCCGTGTTC-3′ (forward) and 5′-TGTCATCATACTTGGCAGGTTTCT-3′ (reverse) for the glyceraldehyde-3-phosphate dehydrogenase gene (*Gapdh*). A comparative analysis of the PCR product amounts was conducted by the comparative cycle threshold (C_T) method using *Gapdh* as a control.

Western blot analysis. The cytosolic fraction was prepared from the 8-month-old *Ggcx* scKO and WT testes by homogenization using radioimmunoprecipitation assay (RIPA) buffer (150 mM NaCl, 50 mM Tris-HCl [pH 8.0], and 1% Triton X-100) and centrifugation at 19,100 × *g* for 20 min at 4°C. These samples were incubated with a sample buffer (100 mM Tris-HCl [pH 6.5], 4% SDS, 20% glycerol, 0.2% bromophenol blue, and 4% 2-mercaptoethanol) at 37°C for 5 min, resolved using 8% SDS-PAGE, and finally electrophoretically transferred onto polyvinylidene difluoride membranes (Merck Millipore, Billerica, MA, USA). The membranes were probed with diluted anti-human GGCX antiserum at a ratio of 1:10,000 (14) and diluted anti-β-actin antibodies at a ratio of 1:10,000 (AC-74; Sigma-Aldrich, St. Louis, MO, USA). Binding of the primary antibodies was detected by diluted horseradish peroxidase (HRP)-conjugated anti-rabbit or anti-mouse immunoglobulin G (IgG) antibodies at a ratio of 1:4,000 (GE Healthcare, Menlo Park, CA). Immunoreactive proteins were visualized using enhanced chemiluminescence (Pierce ECL Plus Western blotting substrate; Thermo Fisher Scientific, Somerset, NJ, USA).

Measurement of serum testosterone levels. Serum testosterone levels of male 2-, 4-, and 8-month-old *Ggcx* scKO and control mice were measured using the rodent testosterone enzyme-linked immunosorbent assay (ELISA) kit (Endocrine Technologies, Newark, CA, USA) according to the manufacturer's instructions.

Hematoxylin and eosin staining. Testes were fixed in 4% paraformaldehyde (PFA) in PBS at 4°C overnight, embedded in paraffin, cut into 5-μm-thick sections, and placed onto glass slides that were coated with 3-aminopropyltriethoxysilane. Using a standard protocol, the slides were deparaffinized, rehydrated, and stained with hematoxylin and eosin (HE).

Transmission electron microscopy. Mice were perfused with a 4% paraformaldehyde solution, and the testes were then resected for subsequent fixation in half-Karnovsky solution (2% paraformaldehyde and 2.5% glutaraldehyde diluted in a 0.067 M cacodylate buffer [pH 7.4]). The specimens were postfixed with OsO_4 and dehydrated with ascending concentrations of acetone prior to epoxy resin embedding as previously described (15). Ultrathin sections of the testes were placed onto grids and stained with uranyl acetate and lead citrate for transmission electron microscopy (TEM) observation as previously described (59).

Immunohistochemistry. Immunohistochemical analysis was performed as previously described (14, 60). The sections were reacted with anti-GGCX rabbit antibody (10 μg/ml) (14), anti-GATA1 rat antibody (10 μg/ml) (catalog number sc-265; Santa Cruz Biotechnology, Santa Cruz, CA, USA), or anti-Cx43 rabbit antibody (0.32 μg/ml) (catalog number C6219; Sigma-Aldrich) for 3 h at room temperature and subsequently incubated for 1 h with HRP-labeled anti-rabbit or -rat IgG at a dilution ratio of 1:200. The sites of HRP were visualized after incubation with a solution that contains diaminobenzidine, H_2O_2, $CoCl_2$-$6H_2O$, and $NiSO_4$-$6H_2O$. As a control, sections were reacted with normal rabbit or rat IgG rather than the primary antibodies.

TUNEL staining. TUNEL staining was performed according to a previously described protocol (60). The sections were deparaffinized, rehydrated, and treated with proteinase K (10 μg/ml) for 15 min at 37°C. After rinsing, the sections were preincubated with terminal deoxynucleotidyltransferase (TdT) buffer (Roche Diagnostics, Penzberg, Germany) for 30 min at room temperature and then reacted with

800 U/ml TdT in TdT buffer that was supplemented with 0.1 mM dithiothreitol, 1.5 mM cobalt chloride, 20 μM dATP, and 1 μM biotin-16-dUTP for 90 min at 37°C. Next, the reaction mixture was washed with 50 mM Tris-HCl buffer (pH 7.5), and the reaction was effectively terminated. Endogenous peroxidase was inactivated by immersing the sections in 0.3% H_2O_2 and methanol for 15 min. The signals were detected immunohistochemically with HRP-conjugated goat antibiotin antibody (catalog number SP-3010; Vector Laboratories, Burlingame, CA, USA).

Analysis of spermatozoa. Sperm samples were collected from the cauda epididymides of 4-month-old *Ggcx* scKO ($n = 3$) and control ($n = 3$) mice and transferred to 400 μl of Toyoda Yokoyama Hoshi (TYH) medium (LSI Medience, Tokyo, Japan) covered with paraffin oil. After incubation at 35°C for 2 h, sperm concentration and morphology were measured using a hemocytometer. The morphological abnormalities of the sperm cells were classified into the following 4 categories: (i) coiled tail, (ii) bent tail, (iii) bent neck, and (iv) abnormal head. Sperm motility was categorized as either hyperactive, straight, irregular, or immotile. At least 100 sperm cells per mouse were counted. Spontaneous acrosome reactions of spermatozoa from WT and *Ggcx* scKO mice were compared by Coomassie staining before and after capacitation incubation.

Statistical analysis. Differences between two groups were analyzed for statistical significance using unpaired Student's *t* test.

Data availability. The data that support the findings of this study are fully available from the corresponding author upon reasonable request.

ACKNOWLEDGMENTS

We thank T. Tsukui and Y. Takahashi for their kind support in the generation of transgenic animals and in the analysis of spermatozoa. We also thank S. Kondo, M. Fujitani, T. Suzuki, N. Sasaki, and W. Sato for their technical assistance.

This work was partially supported by a grant of the Support Project of the Strategic Research Center in Private Universities from the Ministry of Education, Culture, Sports, Science, and Technology, Japan (to Satoshi Inoue); by grants from the Japan Society for the Promotion of Science, Japan (16K09809 [to Kazuhiro Ikeda], 20H03734 [to Kuniko Horie-Inoue], 17H04205 [to Kuniko Horie-Inoue], and 19K07404 [to Sachiko Shiba]); and by the Takeda Science Foundation (to Satoshi Inoue).

We declare no conflicts of interest.

Satoshi Inoue and Sachiko Shiba, conception and design; Sachiko Shiba, Kazuhiro Ikeda, Toshihiko Takeiwa, and Yasuaki Shibata, performance of experiments and development of methodology; Tomoka Hasegawa and Kotaro Azuma, acquisition of data; Norio Amizuka, Tomoaki Tanaka, Kuniko Horie-Inoue, and Takehiko Koji, analysis and interpretation of data; Sachiko Shiba, Kazuhiro Ikeda, and Kuniko Horie-Inoue, writing the original draft of the manuscript; Norio Amizuka, Tomoaki Tanaka, Takehiko Koji, and Satoshi Inoue, reviewing and editing the manuscript.

REFERENCES

1. Azuma K, Ouchi Y, Inoue S. 2014. Vitamin K: novel molecular mechanisms of action and its roles in osteoporosis. Geriatr Gerontol Int 14:1–7. https://doi.org/10.1111/ggi.12060.
2. Nakagawa K, Hirota Y, Sawada N, Yuge N, Watanabe M, Uchino Y, Okuda N, Shimomura Y, Suhara Y, Okano T. 2010. Identification of UBIAD1 as a novel human menaquinone-4 biosynthetic enzyme. Nature 468:117–121. https://doi.org/10.1038/nature09464.
3. Azuma K, Inoue S. 2019. Multiple modes of vitamin K actions in aging-related musculoskeletal disorders. Int J Mol Sci 20:2844. https://doi.org/10.3390/ijms20112844.
4. Azuma K, Tsukui T, Ikeda K, Shiba S, Nakagawa K, Okano T, Urano T, Horie-Inoue K, Ouchi Y, Ikawa M, Inoue S. 2014. Liver-specific γ-glutamyl carboxylase-deficient mice display bleeding diathesis and short life span. PLoS One 9:e88643. https://doi.org/10.1371/journal.pone.0088643.
5. Berkner KL, Pudota BN. 1998. Vitamin K-dependent carboxylation of the carboxylase. Proc Natl Acad Sci U S A 95:466–471. https://doi.org/10.1073/pnas.95.2.466.
6. Parker CH, Morgan CR, Rand KD, Engen JR, Jorgenson JW, Stafford DW. 2014. A conformational investigation of propeptide binding to the integral membrane protein γ-glutamyl carboxylase using nanodisc hydrogen exchange mass spectrometry. Biochemistry 53:1511–1520. https://doi.org/10.1021/bi401536m.
7. Brenner B, Sánchez-Vega B, Wu SM, Lanir N, Stafford DW, Solera J. 1998. A missense mutation in gamma-glutamyl carboxylase gene causes combined deficiency of all vitamin K-dependent blood coagulation factors. Blood 92:4554–4559. https://doi.org/10.1182/blood.V92.12.4554.
8. Spronk HM, Farah RA, Buchanan GR, Vermeer C, Soute BA. 2000. Novel mutation in the gamma-glutamyl carboxylase gene resulting in congenital combined deficiency of all vitamin K-dependent blood coagulation factors. Blood 96:3650–3652. https://doi.org/10.1182/blood.V96.10.3650.
9. Kinoshita H, Nakagawa K, Narusawa K, Goseki-Sone M, Fukushi-Irie M, Mizoi L, Yoshida H, Okano T, Nakamura T, Suzuki T, Inoue S, Orimo H, Ouchi Y, Hosoi T. 2007. A functional single nucleotide polymorphism in the vitamin-K-dependent gamma-glutamyl carboxylase gene (Arg325Gln) is associated with bone mineral density in elderly Japanese women. Bone 40:451–456. https://doi.org/10.1016/j.bone.2006.08.007.
10. Zhu A, Sun H, Raymond RM, Furie BC, Furie B, Bronstein M, Kaufman RJ, Westrick R, Ginsburg D. 2007. Fatal hemorrhage in mice lacking gamma-glutamyl carboxylase. Blood 109:5270–5275. https://doi.org/10.1182/blood-2006-12-064188.
11. Lee NK, Sowa H, Hinoi E, Ferron M, Ahn JD, Confavreux C, Dacquin R, Mee PJ, McKee MD, Jung DY, Zhang Z, Kim JK, Mauvais-Jarvis F, Ducy P, Karsenty G. 2007. Endocrine regulation of energy metabolism by the skeleton. Cell 130:456–469. https://doi.org/10.1016/j.cell.2007.05.047.
12. Ferron M, Hinoi E, Karsenty G, Ducy P. 2008. Osteocalcin differentially regulates beta cell and adipocyte gene expression and affects the development of metabolic diseases in wild-type mice. Proc Natl Acad Sci U S A 105:5266–5270. https://doi.org/10.1073/pnas.0711119105.

13. Ferron M, Wei J, Yoshizawa T, Del Fattore A, DePinho RA, Teti A, Ducy P, Karsenty G. 2010. Insulin signaling in osteoblasts integrates bone remodeling and energy metabolism. Cell 142:296–308. https://doi.org/10.1016/j.cell.2010.06.003.
14. Shiba S, Ikeda K, Azuma K, Hasegawa T, Amizuka N, Horie-Inoue K, Inoue S. 2014. γ-Glutamyl carboxylase in osteoblasts regulates glucose metabolism in mice. Biochem Biophys Res Commun 453:350–355. https://doi.org/10.1016/j.bbrc.2014.09.091.
15. Azuma K, Shiba S, Hasegawa T, Ikeda K, Urano T, Horie-Inoue K, Ouchi Y, Amizuka N, Inoue S. 2015. Osteoblast-specific γ-glutamyl carboxylase-deficient mice display enhanced bone formation with aberrant mineralization. J Bone Miner Res 30:1245–1254. https://doi.org/10.1002/jbmr.2463.
16. Garcia AA, Reitsma PH. 2008. VKORC1 and the vitamin K cycle. Vitam Horm 78:23–33. https://doi.org/10.1016/S0083-6729(07)00002-7.
17. Roncaglioni MC, Soute BA, de Boer-Van den Berg MA, Vermeer C. 1983. Warfarin-induced accumulation of vitamin K-dependent proteins. Comparison between hepatic and non-hepatic tissues. Biochem Biophys Res Commun 114:991–997. https://doi.org/10.1016/0006-291x(83)90658-7.
18. Thijssen HH, Janssen CA, Drittij-Reijnders MJ. 1986. The effect of S-warfarin administration on vitamin K 2,3-epoxide reductase activity in liver, kidney and testis of the rat. Biochem Pharmacol 35:3277–3282. https://doi.org/10.1016/0006-2952(86)90424-7.
19. Ma H, Zhang BL, Liu BY, Shi S, Gao DY, Zhang TC, Shi HJ, Li Z, Shum WW. 2019. Vitamin K2-dependent GGCX and MGP are required for homeostatic calcium regulation of sperm maturation. iScience 14:210–225. https://doi.org/10.1016/j.isci.2019.03.030.
20. Sanyaolu AO, Oremosu AA, Osinubi AA, Vermeer C, Daramola AO. 2019. Warfarin-induced vitamin K deficiency affects spermatogenesis in Sprague-Dawley rats. Andrologia 51:e13416. https://doi.org/10.1111/and.13416.
21. Dutertre M, Rey R, Porteu A, Josso N, Picard JY. 1997. A mouse Sertoli cell line expressing anti-Müllerian hormone and its type II receptor. Mol Cell Endocrinol 136:57–65. https://doi.org/10.1016/s0303-7207(97)00214-1.
22. Lécureuil C, Fontaine I, Crepieux P, Guillou F. 2002. Sertoli and granulosa cell-specific Cre recombinase activity in transgenic mice. Genesis 33:114–118. https://doi.org/10.1002/gene.10100.
23. Griswold MD. 1998. The central role of Sertoli cells in spermatogenesis. Semin Cell Dev Biol 9:411–416. https://doi.org/10.1006/scdb.1998.0203.
24. Wang RA, Nakane PK, Koji T. 1998. Autonomous cell death of mouse male germ cells during fetal and postnatal period. Biol Reprod 58:1250–1256. https://doi.org/10.1095/biolreprod58.5.1250.
25. Koji T, Hishikawa Y. 2003. Germ cell apoptosis and its molecular trigger in mouse testes. Arch Histol Cytol 66:1–16. https://doi.org/10.1679/aohc.66.1.
26. Yomogida K, Ohtani H, Harigae H, Ito E, Nishimune Y, Engel JD, Yamamoto M. 1994. Developmental stage- and spermatogenic cycle-specific expression of transcription factor GATA-1 in mouse Sertoli cells. Development 120:1759–1766.
27. Jarvis S, Elliott DJ, Morgan D, Winston R, Readhead C. 2005. Molecular markers for the assessment of postnatal male germ cell development in the mouse. Hum Reprod 20:108–116. https://doi.org/10.1093/humrep/deh565.
28. Sridharan S, Simon L, Meling DD, Cyr DG, Gutstein DE, Fishman GI, Guillou F, Cooke PS. 2007. Proliferation of adult Sertoli cells following conditional knockout of the gap junctional protein GJA1 (connexin 43) in mice. Biol Reprod 76:804–812. https://doi.org/10.1095/biolreprod.106.059212.
29. Rode K, Weider K, Damm OS, Wistuba J, Langeheine M, Brehm R. 2018. Loss of connexin 43 in Sertoli cells provokes postnatal spermatogonial arrest, reduced germ cell numbers and impaired spermatogenesis. Reprod Biol 18:456–466. https://doi.org/10.1016/j.repbio.2018.08.001.
30. Cheng CY, Mruk DD. 2010. A local autocrine axis in the testes that regulates spermatogenesis. Nat Rev Endocrinol 6:380–395. https://doi.org/10.1038/nrendo.2010.71.
31. Picard J-Y, Josso N. 2019. Persistent Müllerian duct syndrome: an update. Reprod Fertil Dev 31:1240–1245. https://doi.org/10.1071/RD17501.
32. Berndtson WE, Thompson TL. 1990. Changing relationships between testis size, Sertoli cell number and spermatogenesis in Sprague-Dawley rats. J Androl 11:429–435.
33. Ni F-D, Hao S-L, Yang W-X. 2019. Multiple signaling pathways in Sertoli cells: recent findings in spermatogenesis. Cell Death Dis 10:541. https://doi.org/10.1038/s41419-019-1782-z.
34. Wong C-H, Xia W, Lee NPY, Mruk DD, Lee WM, Cheng CY. 2005. Regulation of ectoplasmic specialization dynamics in the seminiferous epithelium by focal adhesion-associated proteins in testosterone-suppressed rat testes. Endocrinology 146:1192–1204. https://doi.org/10.1210/en.2004-1275.
35. Zheng B, Yu J, Guo Y, Gao T, Shen C, Zhang X, Li H, Huang X. 2018. Cellular nucleic acid-binding protein is vital to testis development and spermatogenesis in mice. Reproduction 156:59–69. https://doi.org/10.1530/REP-17-0666.
36. Ahmed N, Yang P, Chen H, Ujjan IA, Haseeb A, Wang L, Soomro F, Faraz S, Sahito B, Ali W, Chen Q. 2018. Characterization of inter-Sertoli cell tight and gap junctions in the testis of turtle: protect the developing germ cells from an immune response. Microb Pathog 123:60–67. https://doi.org/10.1016/j.micpath.2018.06.037.
37. Risley MS, Tan IP, Roy C, Sáez JC. 1992. Cell-, age- and stage-dependent distribution of connexin43 gap junctions in testes. J Cell Sci 103:81–96.
38. Matsuo Y, Nomata K, Eguchi J, Aoki D, Hayashi T, Hishikawa Y, Kanetake H, Shibata Y, Koji T. 2007. Immunohistochemical analysis of connexin43 expression in infertile human testes. Acta Histochem Cytochem 40:69–75. https://doi.org/10.1267/ahc.07001.
39. Rebourcet D, O'Shaughnessy PJ, Monteiro A, Milne L, Cruickshanks L, Jeffrey N, Guillou F, Freeman TC, Mitchell RT, Smith LB. 2014. Sertoli cells maintain Leydig cell number and peritubular myoid cell activity in the adult mouse testis. PLoS One 9:e105687. https://doi.org/10.1371/journal.pone.0105687.
40. Brehm R, Zeiler M, Rüttinger C, Herde K, Kibschull M, Winterhager E, Willecke K, Guillou F, Lécureuil C, Steger K, Konrad L, Biermann K, Failing K, Bergmann M. 2007. A Sertoli cell-specific knockout of connexin43 prevents initiation of spermatogenesis. Am J Pathol 171:19–31. https://doi.org/10.2353/ajpath.2007.061171.
41. Giese S, Hossain H, Markmann M, Chakraborty T, Tchatalbachev S, Guillou F, Bergmann M, Failing K, Weider K, Brehm R. 2012. Sertoli-cell-specific knockout of connexin 43 leads to multiple alterations in testicular gene expression in prepubertal mice. Dis Model Mech 5:895–913. https://doi.org/10.1242/dmm.008649.
42. Yang X, Zhang X, Zhang J, Ji Q, Huang W, Zhang X, Li Y. 2019. Spermatogenesis disorder caused by T-2 toxin is associated with germ cell apoptosis mediated by oxidative stress. Environ Pollut 251:372–379. https://doi.org/10.1016/j.envpol.2019.05.023.
43. Smith LB, Walker WH. 2014. The regulation of spermatogenesis by androgens. Semin Cell Dev Biol 30:2–13. https://doi.org/10.1016/j.semcdb.2014.02.012.
44. Pelletier R-M. 2011. The blood-testis barrier: the junctional permeability, the proteins and the lipids. Prog Histochem Cytochem 46:49–127. https://doi.org/10.1016/j.proghi.2011.05.001.
45. Lyon MF, Glenister PH, Lamoreux ML. 1975. Normal spermatozoa from androgen-resistant germ cells of chimaeric mice and the role of androgen in spermatogenesis. Nature 258:620–622. https://doi.org/10.1038/258620a0.
46. Johnston DS, Russell LD, Friel PJ, Griswold MD. 2001. Murine germ cells do not require functional androgen receptors to complete spermatogenesis following spermatogonial stem cell transplantation. Endocrinology 142:2405–2408. https://doi.org/10.1210/endo.142.6.8317.
47. Tsai M-Y, Yeh S-D, Wang R-S, Yeh S, Zhang C, Lin H-Y, Tzeng C-R, Chang C. 2006. Differential effects of spermatogenesis and fertility in mice lacking androgen receptor in individual testis cells. Proc Natl Acad Sci U S A 103:18975–18980. https://doi.org/10.1073/pnas.0608565103.
48. Wang R-S, Yeh S, Tzeng C-R, Chang C. 2009. Androgen receptor roles in spermatogenesis and fertility: lessons from testicular cell-specific androgen receptor knockout mice. Endocr Rev 30:119–132. https://doi.org/10.1210/er.2008-0025.
49. De Gendt K, Swinnen JV, Saunders PTK, Schoonjans L, Dewerchin M, Devos A, Tan K, Atanassova N, Claessens F, Lécureuil C, Heyns W, Carmeliet P, Guillou F, Sharpe RM, Verhoeven G. 2004. A Sertoli cell-selective knockout of the androgen receptor causes spermatogenic arrest in meiosis. Proc Natl Acad Sci U S A 101:1327–1332. https://doi.org/10.1073/pnas.0308114100.
50. Willems A, Roesl C, Mitchell RT, Milne L, Jeffery N, Smith S, Verhoeven G, Brown P, Smith LB. 2015. Sertoli cell androgen receptor signalling in adulthood is essential for post-meiotic germ cell development. Mol Reprod Dev 82:626–627. https://doi.org/10.1002/mrd.22506.
51. Holdcraft RW, Braun RE. 2004. Androgen receptor function is required in Sertoli cells for the terminal differentiation of haploid spermatids. Development 131:459–467. https://doi.org/10.1242/dev.00957.
52. Licciardello MP, Ringler A, Markt P, Klepsch F, Lardeau C-H, Sdelci S, Schirghuber E, Müller AC, Caldera M, Wagner A, Herzog R, Penz T, Schuster M, Boidol B, Dürnberger G, Folkvaljon Y, Stattin P, Ivanov V, Colinge J, Bock C, Kratochwill K, Menche J, Bennett KL, Kubicek S. 2017. A combinatorial screen of the CLOUD uncovers a synergy targeting the androgen receptor. Nat Chem Biol 13:771–778. https://doi.org/10.1038/nchembio.2382.

53. Lu Q, Gore M, Zhang Q, Camenisch T, Boast S, Casagranda F, Lai C, Skinner MK, Klein R, Matsushima GK, Earp HS, Goff SP, Lemke G. 1999. Tyro-3 family receptors are essential regulators of mammalian spermatogenesis. Nature 398:723–728. https://doi.org/10.1038/19554.
54. Xiong W, Chen Y, Wang H, Wang H, Wu H, Lu Q, Han D. 2008. Gas6 and the Tyro 3 receptor tyrosine kinase subfamily regulate the phagocytic function of Sertoli cells. Reproduction 135:77–87. https://doi.org/10.1530/REP-07-0287.
55. Lemke G, Burstyn-Cohen T. 2010. TAM receptors and the clearance of apoptotic cells. Ann N Y Acad Sci 1209:23–29. https://doi.org/10.1111/j.1749-6632.2010.05744.x.
56. Kanegae Y, Lee G, Sato Y, Tanaka M, Nakai M, Sakaki T, Sugano S, Saito I. 1995. Efficient gene activation in mammalian cells by using recombinant adenovirus expressing site-specific Cre recombinase. Nucleic Acids Res 23:3816–3821. https://doi.org/10.1093/nar/23.19.3816.
57. Ikeda K, Tsukui T, Imazawa Y, Horie-Inoue K, Inoue S. 2012. Conditional expression of constitutively active estrogen receptor α in chondrocytes impairs longitudinal bone growth in mice. Biochem Biophys Res Commun 425:912–917. https://doi.org/10.1016/j.bbrc.2012.07.170.
58. Horie-Inoue K, Takayama K, Bono HU, Ouchi Y, Okazaki Y, Inoue S. 2006. Identification of novel steroid target genes through the combination of bioinformatics and functional analysis of hormone response elements. Biochem Biophys Res Commun 339:99–106. https://doi.org/10.1016/j.bbrc.2005.10.188.
59. Hasegawa T, Yamamoto T, Sakai S, Miyamoto Y, Hongo H, Qiu Z, Abe M, Takeda S, Oda K, de Freitas PHL, Li M, Endo K, Amizuka N. 2019. Histological effects of the combined administration of eldecalcitol and a parathyroid hormone in the metaphyseal trabeculae of ovariectomized rats. J Histochem Cytochem 67:169–184. https://doi.org/10.1369/0022155418806865.
60. Koji T, Kondo S, Hishikawa Y, An S, Sato Y. 2008. In situ detection of methylated DNA by histo endonuclease-linked detection of methylated DNA sites: a new principle of analysis of DNA methylation. Histochem Cell Biol 130:917–925. https://doi.org/10.1007/s00418-008-0487-7.